AN FMRI ACTIVATION METHOD USING COMPLEX DATA

Daniel B. Rowe[1] and Brent R. Logan[2]

[1] Department of Biophysics, [2] Division of Biostatistics
Medical College of Wisconsin 8701 Watertown Plank Rd. Milwaukee, WI 53226

ABSTRACT

In functional magnetic resonance imaging, voxel time courses after Fourier "image reconstruction" are complex valued as a result of phase errors due to magnetic field inhomogeneities. Nearly all fMRI studies derive functional "activation" based on magnitude time courses [1, 2]. Here we propose to directly model the entire complex or bivariate data rather than just the magnitude data. A nonlinear model is used to model activation on the complex signal, and a likelihood ratio test is derived to test for activation at each voxel. We investigate the performance of the model on a simulated dataset.

1. INTRODUCTION

In magnetic resonance imaging, we aim to image the density of "spinning" protons in a real valued object. The equations of Physics work out that the Fourier transform (FT) of the proton spin density (PSD) is a spatial frequency. We will obtain the spatial frequency and perform an inverse Fourier transform (IFT) to obtain the proton spin density. This is done by taking successive measurements in time of a real valued signal, a voltage in a wire. The time axis is transformed to the spatial frequency or k-space axis. This signal is real valued, but it is "complex demodulated." In measuring the signal, there can be either one or two A to D converters. If there is a single A to D converter, successive signal measurements are alternately multiplied by either a cosine or a sine to obtain real (in-phase) and imaginary (quadrature) parts. These two measurements are then shifted either half a step forward or backward to align them. If there are two A to D converters, two measurements are then taken at the same time with one multiplied by a cosine and the other by a sine. This discretely measured complex valued signal is the discrete FT of the PSD. A discrete IFT is applied to the discretely measured signal. The original object or PSD is real valued but due to phase errors, a complex image of PSD's is produced.

After Fourier image reconstruction, each voxel contains a time course of real and imaginary components of the PSD. Magnitude images are produced by taking the square root of the sum of the squares of the real and imaginary parts of the PSD in each voxel at each time point. Nearly all fMRI studies obtain a statistical measure of functional activation based on magnitude image time courses. When this is done, phase information in the data is discarded. A more accurate model should use all the information contained in the data.

Two previous models for complex activation have been proposed [3, 4]; however the first assumes that the phase errors for the baseline and signal are not the same. We extend the second model proposed by Nan and Nowak (1999) to a multiparameter baseline and signal model, formulate the the hypothesis test in terms of contrasts, and estimate the phase angle directly instead of the sine and cosine of the phase angle. We compare the results of this model to a strict magnitude model in terms of thresholded activation maps.

2. MODEL

In MRI/fMRI, we aim to image a real valued object $\rho(x, y)$ and obtain a measured object $\rho_m(x, y)$ by measuring a 2D complex valued signal $s_m(k_x, k_y)$ at spatial frequencies (k_x, k_y). This signal consists of a true complex valued signal $s(k_x, k_y)$ plus a random complex noise term $\delta(k_x, k_y)$ with real and imaginary components that are assumed to be independent and identically normally distributed. Even if there were no phase errors, it is necessary to observe the imaginary parts of this signal because we phase encode for proper image formation. After image reconstruction, we obtain a complex valued measured object plus complex valued noise.

Neglecting the voxel location and focusing on a particular voxel, the complex valued image measured over time in a given voxel is

$$\rho_{mt} \quad = \quad [\rho_{Rt} + \eta_{Rt}] + i[\rho_{It} + \eta_{It}]$$

where $(\eta_{Rt}, \eta_{It})' \sim \mathcal{N}(0, \Sigma)$ and $\Sigma = \sigma^2 I_2$. The dis-

tributional specification is on the real and imaginary parts of the image and not on the magnitude.

A nonlinear multiple regression model is introduced individually for each voxel that includes a phase error θ in which at time t, the measured proton spin density is given by

$$\rho_{mt} \quad = \quad [\rho_t \cos\theta + \eta_{Rt}] + i[\rho_t \sin\theta + \eta_{It}]$$

where $\rho_t = x_t'\beta = \beta_0 + \beta_1 x_{1t} + \cdots + \beta_q x_{qt}$.

In fMRI, we take repeated measurements over time while a subject is performing a task. In each voxel, we compute a measure of association between the observed time course and a preassigned reference function that characterizes the experimental paradigm.

2.1. Magnitude Activation

The typical method to compute activations [1, 2] is to use the magnitude $|\rho_{mt}|$ which is denoted by y_t and written as

$$y_t = \left[(x_t'\beta\cos\theta + \eta_{Rt})^2 + (x_t'\beta\sin\theta + \eta_{It})^2\right]^{\frac{1}{2}}.$$

The phase which may contain some information is discarded. The magnitude data when the signal to noise ratio is large can be approximately modeled [4] as

$$y_t \quad \approx \quad x_t'\beta + \epsilon_t$$

by performing some algebra under the square root and using a Taylor series expansion where $\epsilon_t = \eta_{Rt}\cos\theta + \eta_{It}\sin\theta \sim N(0,\sigma^2)$. This variance σ^2 is the same as that for the real and imaginary parts of the complex image. Alternatively, this can be written as

$$\begin{array}{ccccccc} y & = & X & \beta & + & \epsilon \\ n\times 1 & & n\times(q+1) & (q+1)\times 1 & & n\times 1 \end{array}$$

where $\epsilon \sim \mathcal{N}(0,\sigma^2\Phi)$ and Φ is the temporal correlation matrix, often taken to be $\Phi = I_n$ after suitable preprocessing of the data.

The unconstrained maximum likelihood estimates of the vector of regression coefficients $\hat\beta$ and the error variance $\hat\sigma^2$ are

$$\begin{aligned} \hat\beta_M &= (X'X)^{-1}X'y, \\ \hat\sigma^2_M &= (y - X\hat\beta_M)'(y - X\hat\beta_M)/n. \end{aligned}$$

To construct a generalized likelihood ratio test of the hypothesis $H_0 : C\beta = 0$ vs. $H_a : C\beta \neq 0$, we maximize the likelihood under the constrained null hypothesis. This leads to constrained MLE's

$$\begin{aligned} \tilde\beta_M &= \Psi\hat\beta_M, \\ \tilde\sigma^2_M &= (y - X\tilde\beta_M)'(y - X\tilde\beta_M)/n \end{aligned}$$

where

$$\Psi = I_{q+1} - (X'X)^{-1}C'[C(X'X)^{-1}C']^{-1}C.$$

Then the likelihood ratio statistic is given by

$$-2\log\lambda_M = n\log\left(\frac{\tilde\sigma^2_M}{\hat\sigma^2_M}\right).$$

This has an asymptotic χ^2_1 distribution. Note that magnitude activation maps are usually based on an equivalent representation using t-statistics, but we use the χ^2 representation for comparability with the complex activation model.

2.2. Complex Activation

Alternatively, we can represent the observed data at time point t as a 2×1 vector instead of as a complex number

$$\begin{pmatrix} y_{Rt} \\ y_{It} \end{pmatrix} \quad = \quad \begin{pmatrix} x_t'\beta\cos\theta \\ x_t'\beta\sin\theta \end{pmatrix} \quad + \quad \begin{pmatrix} \eta_{Rt} \\ \eta_{It} \end{pmatrix}$$

with the constraint that $\sin^2\theta + \cos^2\theta = 1$. Note that this can also be written as

$$\begin{array}{ccccccc} y & = & \begin{pmatrix} X & 0 \\ 0 & X \end{pmatrix} & \begin{pmatrix} \beta\cos\theta \\ \beta\sin\theta \end{pmatrix} & + & \eta\,, \\ 2n\times 1 & & 2n\times 2(q+1) & 2(q+1)\times 1 & & 2n\times 1 \end{array}$$

where it is specified that the observed vector of data $y = (y_R', y_I')'$ is the vector of observed real values stacked on the vector of observed complex values and the vector of errors $\eta = (\eta_{Rt}', \eta_{It}')' \sim \mathcal{N}(0, \Sigma\otimes\Phi)$ is similarly defined where $\otimes$ is the Kronecker product.

Due to the multiparameter baseline and signal model along with the direct modeling of the phase angle, this is a generalization of the model by Nan and Nowak where there is only a mean and signal reference function and the cosine and sine of the phase angle is estimated. Note that our model can be reparametrized to yield the Nan and Nowak model for the single parameter baseline and signal setting. As with the magnitude model, we can obtain unrestricted maximum likelihood estimates of the parameters as

$$\begin{aligned} \hat\theta &= \frac{1}{2}\tan^{-1}\left[\frac{2\hat\beta_R'(X'X)\hat\beta_I}{\hat\beta_R'(X'X)\hat\beta_R - \hat\beta_I'(X'X)\hat\beta_I}\right] \\ \hat\beta_C &= \hat\beta_R\cos\hat\theta + \hat\beta_I\sin\hat\theta, \\ \hat\sigma^2_C &= \frac{1}{2n}\left[y - \begin{pmatrix} X & 0 \\ 0 & X \end{pmatrix}\begin{pmatrix} \hat\beta_C\cos\hat\theta \\ \hat\beta_C\sin\hat\theta \end{pmatrix}\right]' \\ &\qquad \left[y - \begin{pmatrix} X & 0 \\ 0 & X \end{pmatrix}\begin{pmatrix} \hat\beta_C\cos\hat\theta \\ \hat\beta_C\sin\hat\theta \end{pmatrix}\right], \end{aligned}$$

where

$$\begin{aligned}\hat{\beta}_R &= (X'X)^{-1}X'y_R,\\ \hat{\beta}_I &= (X'X)^{-1}X'y_I,\end{aligned}$$

The maximum likelihood estimates under the constrained null hypothesis $H_0 : C\beta = 0$ are given by

$$\begin{aligned}\tilde{\theta} &= \frac{1}{2}\tan^{-1}\left[\frac{2\hat{\beta}_R'\Psi(X'X)\hat{\beta}_I}{\hat{\beta}_R'\Psi(X'X)\hat{\beta}_R - \hat{\beta}_I'\Psi(X'X)\hat{\beta}_I}\right]\\ \tilde{\beta}_C &= \Psi[\hat{\beta}_R\cos\tilde{\theta} + \hat{\beta}_I\sin\tilde{\theta}],\\ \tilde{\sigma}_C^2 &= \frac{1}{2n}\left[y - \begin{pmatrix} X & 0\\ 0 & X\end{pmatrix}\begin{pmatrix}\tilde{\beta}_C\cos\tilde{\theta}\\ \tilde{\beta}_C\sin\tilde{\theta}\end{pmatrix}\right]'\\ &\quad\left[y - \begin{pmatrix} X & 0\\ 0 & X\end{pmatrix}\begin{pmatrix}\tilde{\beta}_C\cos\tilde{\theta}\\ \tilde{\beta}_C\sin\tilde{\theta}\end{pmatrix}\right].\end{aligned}$$

where Ψ is as previously defined for the magnitude model. Previous models were not formulated in terms of contrasts.

Then the generalized likelihood ratio statistic for the complex activation model is

$$-2\log\lambda_C = 2n\log\left(\frac{\tilde{\sigma}_C^2}{\hat{\sigma}_C^2}\right),$$

which, like the magnitude model LRT, also has an asymptotic χ_1^2 distribution.

3. FMRI SIMULATION

Data is generated to simulate a bilateral finger tapping fMRI block design experiment with $n = 256$ points where the true motor activation structure is known so that the two activation methods can be evaluated. A 128×128 slice is selected for analysis within which two 7×7 ROI's as lightened in Figure 1 are designated to have activation.

For this slice, simulated FMRI data is constructed according to a regression model which consists of an intercept, a time trend for all voxels but also a reference function for voxels in each ROI which is related to a $8 \times (16\text{on} + 16\text{off})$ TR block experimental design.

Estimated complex model voxel coefficient values of $(1.63905, .00001, .05870)'$ and variance .00241 were extracted from a significantly active voxel in a real fMRI bilateral finger tapping experiment. The estimated phase was extracted for the entire image of interest. Additional research (not shown) indicated that the models perform similarly for high signal to noise ratios (SNR). Here we illustrate the differences for low SNR. Note that the magnitude of β_0 observed in the real dataset is generally much much larger than β_1 or β_2, indicating that it is the dominant feature in the SNR.

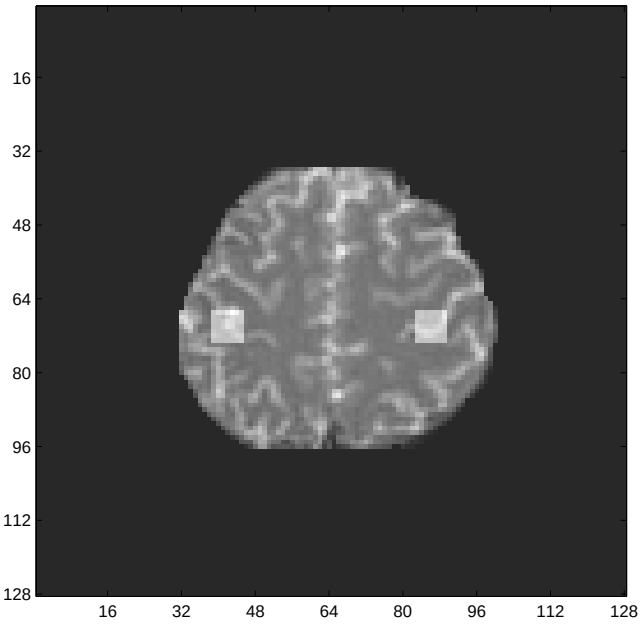

Fig. 1. Anatomical with ROI's.

Therefore for fixed variance, we parametrize the SNR by setting β_0 so that the ratio SNR$= \beta_0/\sigma = 1$. Outside the ROI the simulation true reference coefficient value was set to zero. Inside each ROI, the regression coefficients associated with the reference function are chosen to have an activation region that was $.75 * .05870$ times a normal hill with a variance of 2 and unit height plus $.25 * .05870$. This type of simulated activation has been successfully used before [5] and has the property of the largest effect in the center and smaller effects towards the edge.

The images of $-2\ln\lambda$ for the magnitude data and complex data are given in Figures 2 and 3, each thresholded at a false discovery rate (FDR) of 5% [6, 5]. Since both of these have approximately the same χ_1^2 distribution, these images indicate that the complex model has greater sensitivity to the activation present in the two ROI's, and is therefore preferred. To highlight this difference in activation, the image in Figure 4 was formed from complex model activation minus magnitude model activation.

4. CONCLUSION

A complex data fMRI activation model that uses phase information was presented as an alternative to the typical magnitude data model. Activation statistics were derived from generalized likelihood ratio tests for both models allowing for contrasts. Activation from both

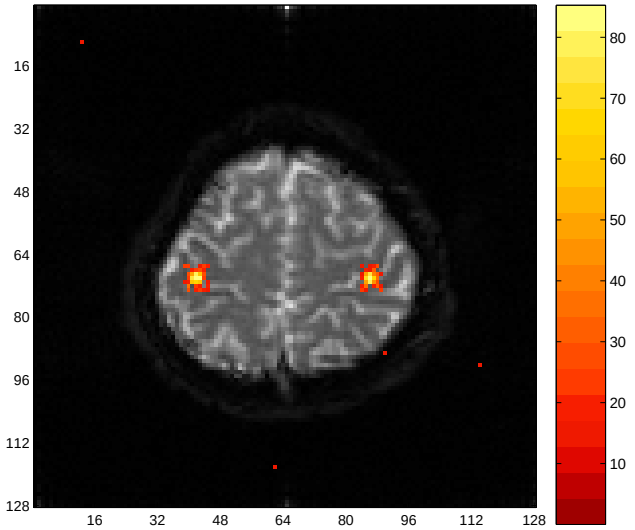

Fig. 2. $-2\ln\lambda$ statistics for magnitude data.

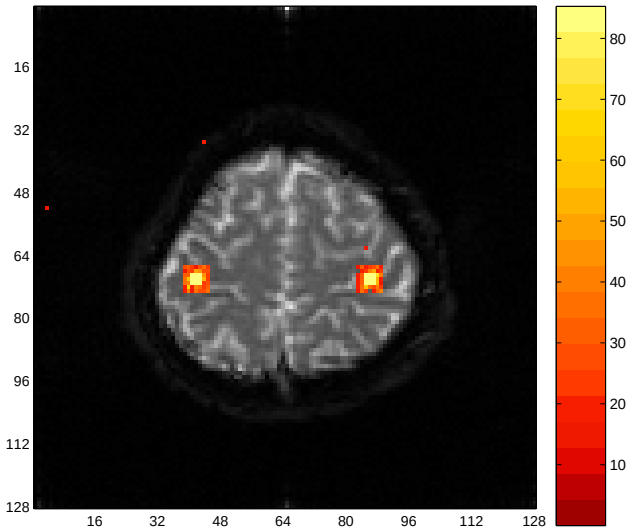

Fig. 3. $-2\ln\lambda$ statistics for complex data.

models were presented for a simulated dataset, illustrating that for smaller signal to noise ratios, the complex activation model demonstrated superior power of detection over the magnitude activation model.

5. REFERENCES

[1] P. Bandettini, A. Jesmanowicz, E. Wong, and J.S. Hyde, "Processing strategies for time-course data sets in functional MRI of the human brain," Magnetic Resonance in Medicine, vol. 30, no. 2, pp. 161–173, 1993.

[2] R.W. Cox, A. Jesmanowicz, and J.S. Hyde, "Real-time functional magnetic resonance imaging," Magnetic Resonance in Medicine, vol. 33, no. 2, pp. 230–236, 1995.

[3] S. Lai and G.H. Glover, "Detection of BOLD fMRI signals using complex data," Proceedings of the ISMRM, p. 1671, 1997.

[4] F.Y. Nan and R.D. Nowak, "Generalized likelihood ratio detection for fMRI using complex data," IEEE Transactions on Medical Imaging, vol. 18, no. 4, pp. 320–329, 1999.

[5] B.R. Logan and D.B. Rowe, "An evaluation of thresholding techniques in fMRI analysis.," Neuroimage, 2004, Forthcoming.

[6] Y. Benjamini and Y. Hochberg, "Controlling the false discovery rate: A practical and powerful approach to multiple testing," Journal of the Royal Statistical Society B, vol. 57, pp. 289–300, 1995.

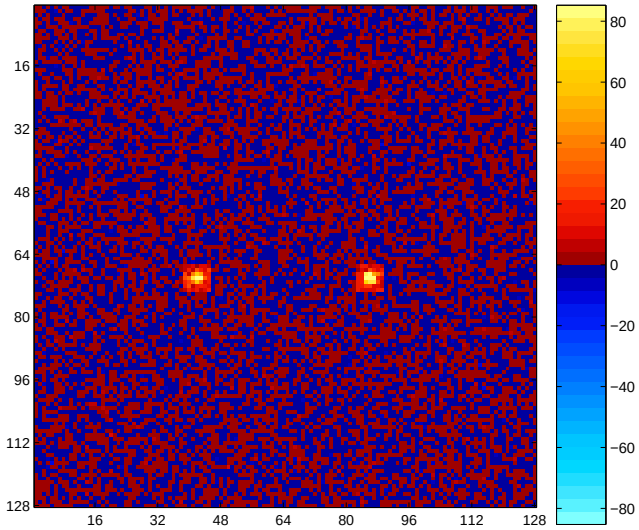

Fig. 4. Activation statistic differences.